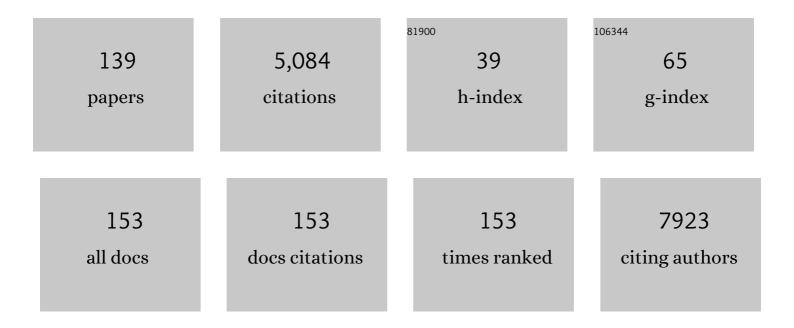
List of Publications by Year in descending order

Source: https://exaly.com/author-pdf/5155260/publications.pdf Version: 2024-02-01



ΙΔΝ ΡΗΟΕΜΔΝΝ

#	Article	IF	CITATIONS
1	Evaluating the Stability of Co ₂ P Electrocatalysts in the Hydrogen Evolution Reaction for Both Acidic and Alkaline Electrolytes. ACS Energy Letters, 2018, 3, 1360-1365.	17.4	291
2	CO oxidation by Pd supported on CeO2(100) and CeO2(111) facets. Applied Catalysis B: Environmental, 2019, 243, 36-46.	20.2	231
3	Atomically Dispersed Pd–O Species on CeO ₂ (111) as Highly Active Sites for Low-Temperature CO Oxidation. ACS Catalysis, 2017, 7, 6887-6891.	11.2	208
4	Two birds with one stone: dual grain-boundary and interface passivation enables >22% efficient inverted methylammonium-free perovskite solar cells. Energy and Environmental Science, 2021, 14, 5875-5893.	30.8	180
5	Carbide-derived carbon aerogels with tunable pore structure as versatile electrode material in high power supercapacitors. Carbon, 2017, 113, 283-291.	10.3	171
6	ZrO ₂ Is Preferred over TiO ₂ as Support for the Ru-Catalyzed Hydrogenation of Levulinic Acid to γ-Valerolactone. ACS Catalysis, 2016, 6, 5462-5472.	11.2	169
7	Trimodal Porous Hierarchical SSZ-13 Zeolite with Improved Catalytic Performance in the Methanol-to-Olefins Reaction. ACS Catalysis, 2016, 6, 2163-2177.	11.2	116
8	Temperature-Dependent Kinetic Studies of the Chlorine Evolution Reaction over RuO ₂ (110) Model Electrodes. ACS Catalysis, 2017, 7, 2403-2411.	11.2	111
9	Ex Situ and Operando Studies on the Role of Copper in Cu-Promoted SiO ₂ –MgO Catalysts for the Lebedev Ethanol-to-Butadiene Process. ACS Catalysis, 2015, 5, 6005-6015.	11.2	95
10	Low-temperature plasma-enhanced atomic layer deposition of 2-D MoS ₂ : large area, thickness control and tuneable morphology. Nanoscale, 2018, 10, 8615-8627.	5.6	90
11	The Origin of High Activity of Amorphous MoS ₂ in the Hydrogen Evolution Reaction. ChemSusChem, 2019, 12, 4383-4389.	6.8	90
12	The electronic structure of transition metal oxides for oxygen evolution reaction. Journal of Materials Chemistry A, 2021, 9, 19465-19488.	10.3	90
13	Interplay between Surface Chemistry, Precursor Reactivity, and Temperature Determines Outcome of ZnS Shelling Reactions on CuInS ₂ Nanocrystals. Chemistry of Materials, 2018, 30, 2400-2413.	6.7	85
14	Stability of Pt/γ-Al ₂ O ₃ Catalysts in Lignin and Lignin Model Compound Solutions under Liquid Phase Reforming Reaction Conditions. ACS Catalysis, 2013, 3, 464-473.	11.2	82
15	Role of Adsorbed Water on Charge Carrier Dynamics in Photoexcited TiO ₂ . Journal of Physical Chemistry C, 2017, 121, 7514-7524.	3.1	82
16	Understanding the Charge Storage Mechanism to Achieve High Capacity and Fast Ion Storage in Sodiumâ€Ion Capacitor Anodes by Using Electrospun Nitrogenâ€Đoped Carbon Fibers. Advanced Functional Materials, 2019, 29, 1902858.	14.9	79
17	Increased activity in the oxygen evolution reaction by Fe ⁴⁺ -induced hole states in perovskite La _{1â^'x} Sr _x FeO ₃ . Journal of Materials Chemistry A, 2020, 8, 4407-4415.	10.3	78
18	Ni ³⁺ -Induced Hole States Enhance the Oxygen Evolution Reaction Activity of Ni _{<i>x</i>} Co _{3–<i>x</i>} O ₄ Electrocatalysts. Chemistry of Materials, 2019, 31, 7618-7625.	6.7	76

#	Article	IF	CITATIONS
19	Cu2O photoelectrodes for solar water splitting: Tuning photoelectrochemical performance by controlled faceting. Solar Energy Materials and Solar Cells, 2015, 141, 178-186.	6.2	72
20	Electronic Effects Determine the Selectivity of Planar Au–Cu Bimetallic Thin Films for Electrochemical CO ₂ Reduction. ACS Applied Materials & Interfaces, 2019, 11, 16546-16555.	8.0	71
21	Quantitative 3D Fluorescence Imaging of Single Catalytic Turnovers Reveals Spatiotemporal Gradients in Reactivity of Zeolite H-ZSM-5 Crystals upon Steaming. Journal of the American Chemical Society, 2015, 137, 6559-6568.	13.7	69
22	High‣fficiency InPâ€Based Photocathode for Hydrogen Production by Interface Energetics Design and Photon Management. Advanced Functional Materials, 2016, 26, 679-686.	14.9	69
23	Reaction Mechanism of the Oxidation of HCl over RuO ₂ (110). Journal of Physical Chemistry C, 2008, 112, 9966-9969.	3.1	68
24	Elucidating the electronic structure of CuWO ₄ thin films for enhanced photoelectrochemical water splitting. Journal of Materials Chemistry A, 2019, 7, 11895-11907.	10.3	67
25	Enhanced Photoresponse of FeS ₂ Films: The Role of Marcasite–Pyrite Phase Junctions. Advanced Materials, 2016, 28, 9602-9607.	21.0	64
26	Enhancing the electrocatalytic activity of 2H-WS ₂ for hydrogen evolution <i>via</i> defect engineering. Physical Chemistry Chemical Physics, 2019, 21, 6071-6079.	2.8	60
27	Edge-Site Nanoengineering of WS ₂ by Low-Temperature Plasma-Enhanced Atomic Layer Deposition for Electrocatalytic Hydrogen Evolution. Chemistry of Materials, 2019, 31, 5104-5115.	6.7	57
28	Porous nitrogen-doped carbon/carbon nanocomposite electrodes enable sodium ion capacitors with high capacity and rate capability. Nano Energy, 2020, 67, 104240.	16.0	56
29	Probing CO ₂ Reduction Pathways for Copper Catalysis Using an Ionic Liquid as a Chemical Trapping Agent. Angewandte Chemie - International Edition, 2020, 59, 18095-18102.	13.8	56
30	In situ studies of the oxidation of HCl over RuO2 model catalysts: Stability and reactivity. Journal of Catalysis, 2010, 272, 169-175.	6.2	54
31	Mn promotion of rutile TiO2-RuO2 anodes for water oxidation in acidic media. Applied Catalysis B: Environmental, 2020, 261, 118225.	20.2	53
32	Intergrowth Structure and Aluminium Zoning of a Zeolite ZSMâ€5 Crystal as Resolved by Synchrotronâ€Based Micro Xâ€Ray Diffraction Imaging. Angewandte Chemie - International Edition, 2013, 52, 13382-13386.	13.8	51
33	Effects of the Functionalization of the Ordered Mesoporous Carbon Support Surface on Iron Catalysts for the Fischer–Tropsch Synthesis of Lower Olefins. ChemCatChem, 2017, 9, 620-628.	3.7	50
34	Synthesis of hierarchical zeolites using an inexpensive mono-quaternary ammonium surfactant as mesoporogen. Chemical Communications, 2014, 50, 14658-14661.	4.1	48
35	Comparing the Intrinsic HER Activity of Transition Metal Dichalcogenides: Pitfalls and Suggestions. ACS Energy Letters, 2021, 6, 2619-2625.	17.4	47
36	Effect of proximity and support material on deactivation of bifunctional catalysts for the conversion of synthesis gas to olefins and aromatics. Catalysis Today, 2020, 342, 161-166.	4.4	46

#	Article	IF	CITATIONS
37	Large area, patterned growth of 2D MoS ₂ and lateral MoS ₂ –WS ₂ heterostructures for nano- and opto-electronic applications. Nanotechnology, 2020, 31, 255603.	2.6	46
38	Unraveling the Role of Lithium in Enhancing the Hydrogen Evolution Activity of MoS ₂ : Intercalation versus Adsorption. ACS Energy Letters, 2019, 4, 1733-1740.	17.4	45
39	In situ spectroscopic investigation of oxidative dehydrogenation and disproportionation of benzyl alcohol. Physical Chemistry Chemical Physics, 2013, 15, 12147.	2.8	43
40	Electronic Structure and Interface Energetics of CuBi ₂ O ₄ Photoelectrodes. Journal of Physical Chemistry C, 2020, 124, 22416-22425.	3.1	39
41	Correlating the electronic structure of perovskite La1â^'Sr CoO3 with activity for the oxygen evolution reaction: The critical role of Co 3d hole state. Journal of Energy Chemistry, 2022, 65, 637-645.	12.9	39
42	Electrolyte Effects on the Stability of Niâ~'Mo Cathodes for the Hydrogen Evolution Reaction. ChemSusChem, 2019, 12, 3491-3500.	6.8	37
43	Water-Dispersible Copper Sulfide Nanocrystals via Ligand Exchange of 1-Dodecanethiol. Chemistry of Materials, 2019, 31, 541-552.	6.7	37
44	Nanoscale Hybrid Amorphous/Graphitic Carbon as Key Towards Nextâ€Generation Carbonâ€Based Oxidative Dehydrogenation Catalysts. Angewandte Chemie - International Edition, 2021, 60, 5898-5906.	13.8	37
45	Potassium hydride-intercalated graphite as an efficient heterogeneous catalyst for ammonia synthesis. Nature Catalysis, 2022, 5, 222-230.	34.4	37
46	Controlled Synthesis of Phaseâ€Pure Zeolitic Imidazolate Framework Coâ€ZIFâ€9. European Journal of Inorganic Chemistry, 2015, 2015, 1625-1630.	2.0	36
47	Fluoride-assisted synthesis of bimodal microporous SSZ-13 zeolite. Chemical Communications, 2016, 52, 3227-3230.	4.1	36
48	Stability of CoP _{<i>x</i>} Electrocatalysts in Continuous and Interrupted Acidic Electrolysis of Water. ChemElectroChem, 2018, 5, 1230-1239.	3.4	35
49	Low-Temperature Phase-Controlled Synthesis of Titanium Di- and Tri-sulfide by Atomic Layer Deposition. Chemistry of Materials, 2019, 31, 9354-9362.	6.7	35
50	Investigation of the stability of NiFe-(oxy)hydroxide anodes in alkaline water electrolysis under industrially relevant conditions. Catalysis Science and Technology, 2020, 10, 5593-5601.	4.1	35
51	Catalytic Hydrogenation of Renewable Levulinic Acid to γ-Valerolactone: Insights into the Influence of Feed Impurities on Catalyst Performance in Batch and Flow Reactors. ACS Sustainable Chemistry and Engineering, 2020, 8, 5903-5919.	6.7	35
52	The Influence of the Ligand in the Iridium Mediated Electrocatalyic Water Oxidation. ACS Catalysis, 2020, 10, 4398-4410.	11.2	32
53	On the Stability of Co ₃ O ₄ Oxygen Evolution Electrocatalysts in Acid. ChemCatChem, 2021, 13, 459-467.	3.7	32
54	CO ₂ Hydrogenation to Higher Alcohols over K-Promoted Bimetallic Fe–In Catalysts on a Ce–ZrO ₂ Support. ACS Sustainable Chemistry and Engineering, 2021, 9, 6235-6249.	6.7	32

#	Article	IF	CITATIONS
55	Electrochemical stability of RuO2(110)/Ru(0001) model electrodes in the oxygen and chlorine evolution reactions. Electrochimica Acta, 2020, 336, 135713.	5.2	30
56	Large Zeolite Hâ€ZSMâ€5 Crystals as Models for the Methanolâ€ŧoâ€Hydrocarbons Process: Bridging the Gap between Singleâ€Particle Examination and Bulk Catalyst Analysis. Chemistry - A European Journal, 2013, 19, 8533-8542.	3.3	29
57	Metalâ€Organic Frameworks as Catalyst Supports: Influence of Lattice Disorder on Metal Nanoparticle Formation. Chemistry - A European Journal, 2018, 24, 7498-7506.	3.3	29
58	Stabilization effects in binary colloidal Cu and Ag nanoparticle electrodes under electrochemical CO ₂ reduction conditions. Nanoscale, 2021, 13, 4835-4844.	5.6	29
59	Mesoporous High-Entropy Oxide Thin Films: Electrocatalytic Water Oxidation on High-Surface-Area Spinel (Cr _{0.2} Mn _{0.2} Fe _{0.2} Co _{0.2} Ni _{0.2}) ₃ O Electrodes. ACS Applied Energy Materials. 2022. 5. 717-730.	_{4<!--</td--><td>29 sub></td>}	29 sub>
60	Dynamic response of chlorine atoms on a RuO2(110) model catalyst surface. Physical Chemistry Chemical Physics, 2010, 12, 15358.	2.8	28
61	Promoted Iron Nanocrystals Obtained via Ligand Exchange as Active and Selective Catalysts for Synthesis Gas Conversion. ACS Catalysis, 2017, 7, 5121-5128.	11.2	26
62	Hydrogen-Promoted Chlorination of RuO ₂ (110). Journal of Physical Chemistry C, 2010, 114, 10901-10909.	3.1	25
63	Role of Dissociatively Adsorbed Water on the Formation of Shallow Trapped Electrons in TiO ₂ Photocatalysts. Journal of Physical Chemistry C, 2017, 121, 10153-10162.	3.1	24
64	Influence of Reduced Cu Surface States on the Photoelectrochemical Properties of CuBi ₂ O ₄ . ACS Applied Energy Materials, 2019, 2, 6866-6874.	5.1	23
65	Towards a quantitative determination of strain in Bragg Coherent X-ray Diffraction Imaging: artefacts and sign convention in reconstructions. Scientific Reports, 2019, 9, 17357.	3.3	23
66	High-entropy transition metal chalcogenides as electrocatalysts for renewable energy conversion. Current Opinion in Electrochemistry, 2022, 34, 101010.	4.8	22
67	Promoting oxygen evolution of IrO2 in acid electrolyte by Mn. Electrochimica Acta, 2021, 366, 137448.	5.2	21
68	Optimization of SnO ₂ electron transport layer for efficient planar perovskite solar cells with very low hysteresis. Materials Advances, 2022, 3, 456-466.	5.4	20
69	Imaging the effect of a hydrothermal treatment on the pore accessibility and acidity of large ZSM-5 zeolite crystals by selective staining. Catalysis Science and Technology, 2013, 3, 1208-1214.	4.1	19
70	Probing the Influence of SSZâ€13 Zeolite Pore Hierarchy in Methanolâ€toâ€Olefins Catalysis by Using Nanometer Accuracy by Stochastic Chemical Reactions Fluorescence Microscopy and Positron Emission Profiling. ChemCatChem, 2017, 9, 3470-3477.	3.7	19
71	Interfacial charge transfer in Pt-loaded TiO2 P25 photocatalysts studied by in-situ diffuse reflectance FTIR spectroscopy of adsorbed CO. Journal of Photochemistry and Photobiology A: Chemistry, 2019, 370, 84-88.	3.9	19
72	A spectrochemometric approach to tautomerism and hydrogen-bonding in 3-acyltetronic acids. Journal of Molecular Structure, 2006, 790, 80-88.	3.6	18

#	Article	IF	CITATIONS
73	Electrospun Metal Oxide Nanofibres for the Assessment of Catalyst Morphological Stability under Harsh Reaction Conditions. ChemCatChem, 2013, 5, 2621-2626.	3.7	18
74	Recent advances in secondary ion mass spectrometry of solid acid catalysts: large zeolite crystals under bombardment. Physical Chemistry Chemical Physics, 2014, 16, 5465-5474.	2.8	18
75	Enhanced CO2 methanation activity over La2-xCexNiO4 perovskite-derived catalysts: Understanding the structure-performance relationships. Chemical Engineering Journal, 2021, 426, 131760.	12.7	18
76	Tandem promotion of iron catalysts by sodium-sulfur and nitrogen-doped carbon layers on carbon nanotube supports for the Fischer-Tropsch to olefins synthesis. Applied Catalysis A: General, 2018, 568, 213-220.	4.3	17
77	Pinpointing the active species of the Cu(DAT) catalyzed oxygen reduction reaction. Physical Chemistry Chemical Physics, 2018, 20, 19625-19634.	2.8	17
78	Template-Free Nanostructured Fluorine-Doped Tin Oxide Scaffolds for Photoelectrochemical Water Splitting. ACS Applied Materials & Interfaces, 2019, 11, 36485-36496.	8.0	17
79	Facile Synthesis of Sulfur ontaining Transition Metal (Mn, Fe, Co, and Ni) (Hydr)oxides for Efficient Oxygen Evolution Reaction. ChemCatChem, 2020, 12, 710-716.	3.7	17
80	Predoped Oxygenated Defects Activate Nitrogen-Doped Graphene for the Oxygen Reduction Reaction. ACS Catalysis, 2022, 12, 173-182.	11.2	17
81	One-dimensional confinement in heterogeneous catalysis: Trapped oxygen on RuO2(110) model catalysts. Surface Science, 2012, 606, L69-L73.	1.9	15
82	On the Formation of Cd–Zn Sulfide Photocatalysts from Insoluble Hydroxide Precursors. Inorganic Chemistry, 2015, 54, 9491-9498.	4.0	14
83	Xâ€ray Excited Optical Fluorescence and Diffraction Imaging of Reactivity and Crystallinity in a Zeolite Crystal: Crystallography and Molecular Spectroscopy in One. Angewandte Chemie - International Edition, 2016, 55, 7496-7500.	13.8	14
84	On the origin of the photocurrent of electrochemically passivated p-InP(100) photoelectrodes. Physical Chemistry Chemical Physics, 2018, 20, 14242-14250.	2.8	14
85	Crystallographic orientation of facets and planar defects in functional nanostructures elucidated by nano-focused coherent diffractive X-ray imaging. Nanoscale, 2018, 10, 4833-4840.	5.6	14
86	Marrying SPR excitation and metal–support interactions: unravelling the contribution of active surface species in plasmonic catalysis. Nanoscale, 2018, 10, 8560-8568.	5.6	14
87	Twin boundary migration in an individual platinum nanocrystal during catalytic CO oxidation. Nature Communications, 2021, 12, 5385.	12.8	14
88	On the Homogeneity of a Cobalt-Based Water Oxidation Catalyst. ACS Catalysis, 2022, 12, 4597-4607.	11.2	14
89	Adsorption of chlorine on Ru(0001)—A combined density functional theory and quantitative low energy electron diffraction study. Surface Science, 2012, 606, 297-304.	1.9	13
90	Bottlenecks limiting efficiency of photocatalytic water reduction by mixed Cd-Zn sulfides/Pt-TiO 2 composites. Applied Catalysis B: Environmental, 2016, 198, 16-24.	20.2	13

#	Article	IF	CITATIONS
91	Solar Driven Energy Conversion Applications Based on 3C-SiC. Materials Science Forum, 0, 858, 1028-1031.	0.3	13
92	Assessment of the Location of Pt Nanoparticles in Pt/zeolite Y/γâ€Al ₂ O ₃ Composite Catalysts. ChemCatChem, 2020, 12, 615-622.	3.7	13
93	Controlling pore size and pore functionality in sp ² -conjugated microporous materials by precursor chemistry and salt templating. Journal of Materials Chemistry A, 2020, 8, 21680-21689.	10.3	13
94	Efficient palladium catalysis for the upgrading of itaconic and levulinic acid to 2-pyrrolidones followed by their vinylation into value-added monomers. Green Chemistry, 2020, 22, 4532-4540.	9.0	13
95	Hybrid Oleate–Iodide Ligand Shell for Air-Stable PbSe Nanocrystals and Superstructures. Chemistry of Materials, 2019, 31, 5808-5815.	6.7	12
96	Near infrared emission spectrum of H13CN. Journal of Molecular Spectroscopy, 2010, 262, 75-81.	1.2	11
97	Nanoweb Surfaceâ€Mounted Metal–Organic Framework Films with Tunable Amounts of Acid Sites as Tailored Catalysts. Chemistry - A European Journal, 2020, 26, 691-698.	3.3	11
98	Hydrogen-efficient non-oxidative transformation of methanol into dimethoxymethane over a tailored bifunctional Cu catalyst. Sustainable Energy and Fuels, 2021, 5, 117-126.	4.9	11
99	Imaging the facet surface strain state of supported multi-faceted Pt nanoparticles during reaction. Nature Communications, 2022, 13, .	12.8	11
100	<i>In situ</i> structural evolution of single particle model catalysts under ambient pressure reaction conditions. Nanoscale, 2019, 11, 331-338.	5.6	10
101	Structure and Basicity of Microporous Titanosilicate ETS-10 and Vanadium-Containing ETS-10. Journal of Physical Chemistry C, 2012, 116, 17124-17133.	3.1	9
102	A comprehensive comparative study of CO2-resistance and oxygen permeability of 60Âwt % Ce0.8M0.2O2– (M = La, Pr, Nd, Sm, Gd) - 40Âwt % La0.5Sr0.5Fe0.8Cu0.2O3– dual-phase membranes. Journa of Membrane Science, 2021, 639, 119783.	al 8.2	9
103	Thickness and Morphology Dependent Electrical Properties of ALDâ€Synthesized MoS ₂ FETs. Advanced Electronic Materials, 2022, 8, .	5.1	9
104	"Extracting―the Key Fragment in ETSâ€10 Crystallization and Its Application in AMâ€6 Assembly. Chemistry A European Journal, 2012, 18, 12078-12084.	- 3.3	8
105	Influence of Local Environments in Pores of Different Size on the Catalytic Liquid-Phase Oxidation of <scp>d</scp> -Glucose by Au Nanoparticles Supported on Nanoporous Carbon. ACS Applied Nano Materials, 2020, 3, 7695-7703.	5.0	8
106	Identification of Photoexcited Electron Relaxation in a Cobalt Phosphide Modified Carbon Nitride Photocatalyst. ChemPhotoChem, 2021, 5, 330-334.	3.0	8
107	On the Contact Optimization of ALD-Based MoS ₂ FETs: Correlation of Processing Conditions and Interface Chemistry with Device Electrical Performance. ACS Applied Electronic Materials, 2021, 3, 3185-3199.	4.3	8
108	Toward Understanding the Shortâ€Circuit Current Loss in Perovskite Solar Cells with 2D Passivation Layers. Solar Rrl, 2022, 6, .	5.8	8

#	Article	IF	CITATIONS
109	Synchrotron based operando surface Xâ€ray scattering study towards structure–activity relationships of model electrocatalysts. ChemistrySelect, 2016, 1, 1104-1108.	1.5	7
110	Synthesis, Physicochemical Characterization, and Cytotoxicity Assessment of CeO ₂ Nanoparticles with Different Morphologies. European Journal of Inorganic Chemistry, 2017, 2017, 3184-3190.	2.0	7
111	Reactor for nano-focused x-ray diffraction and imaging under catalytic in situ conditions. Review of Scientific Instruments, 2017, 88, 093902.	1.3	7
112	Ligand-free ZnS nanoparticles: as easy and green as it gets. Chemical Communications, 2020, 56, 8707-8710.	4.1	7
113	A Selective Copper Based Oxygen Reduction Catalyst for the Electrochemical Synthesis of H 2 O 2 at Neutral pH. ChemElectroChem, 2022, 9, .	3.4	7
114	Xâ€ray Excited Optical Fluorescence and Diffraction Imaging of Reactivity and Crystallinity in a Zeolite Crystal: Crystallography and Molecular Spectroscopy in One. Angewandte Chemie, 2016, 128, 7622-7626.	2.0	6
115	Efficient and Highly Transparent Ultraâ€Thin Nickelâ€Iron Oxyâ€hydroxide Catalyst for Oxygen Evolution Prepared by Successive Ionic Layer Adsorption and Reaction. ChemPhotoChem, 2019, 3, 1050-1054.	3.0	6
116	Probing CO 2 Reduction Pathways for Copper Catalysis Using an Ionic Liquid as a Chemical Trapping Agent. Angewandte Chemie, 2020, 132, 18251-18258.	2.0	6
117	Continuous scanning for Bragg coherent X-ray imaging. Scientific Reports, 2020, 10, 12760.	3.3	6
118	Stability of Colloidal Iron Oxide Nanoparticles on Titania and Silica Support. Chemistry of Materials, 2020, 32, 5226-5235.	6.7	6
119	Reversible hydrogenation restores defected graphene to graphene. Science China Chemistry, 2021, 64, 1047-1056.	8.2	6
120	Synthesis and Morphology Control of AMâ€6 Nanofibers with Tailored â€Vâ€Oâ€Vâ€Intermediates. Chemistry - A European Journal, 2013, 19, 14200-14204.	[\] 3.3	5
121	Elucidation of the Structure of a Thiol Functionalized Cu-tmpa Complex Anchored to Gold via a Self-Assembled Monolayer. Inorganic Chemistry, 2019, 58, 13007-13019.	4.0	5
122	Electroless Nanoplating of Iridium: Templateâ€Assisted Nanotube Deposition for the Continuous Flow Reduction of 4â€Nitrophenol. ChemElectroChem, 2020, 7, 3496-3507.	3.4	5
123	Cu Electrodeposition on Nanostructured MoS ₂ and WS ₂ and Implications for HER Active Site Determination. Journal of the Electrochemical Society, 2020, 167, 116517.	2.9	5
124	Synthesis of edge-enriched WS2 on high surface area WS2 framework by atomic layer deposition for electrocatalytic hydrogen evolution reaction. Journal of Vacuum Science and Technology A: Vacuum, Surfaces and Films, 2020, 38, .	2.1	4
125	Facetâ€Dependent Strain Determination in Electrochemically Synthetized Platinum Model Catalytic Nanoparticles. Small, 2021, 17, e2007702.	10.0	4
126	Ru on Nâ€doped Carbon for the Selective Hydrogenolysis of Sugars and Sugar Alcohols. ChemCatChem, 0, , .	3.7	4

#	Article	IF	CITATIONS
127	Nanoskaliger hybrider amorph/graphitischer Kohlenstoff als Schlüssel zur nÃ e hsten Generation von kohlenstoffbasierten Katalysatoren für oxidative Dehydrierungen. Angewandte Chemie, 2021, 133, 5962-5971.	2.0	3
128	A Heterogenized Copper Phenanthroline System to Catalyze the Oxygen Reduction Reaction. ChemElectroChem, 2022, 9, .	3.4	3
129	The Origin of High Activity of Amorphous MoS 2 in the Hydrogen Evolution Reaction. ChemSusChem, 2019, 12, 4336-4336.	6.8	2
130	Phosphate-assisted efficient oxygen evolution over finely dispersed cobalt particles supported on graphene. Catalysis Science and Technology, 2021, 11, 1039-1048.	4.1	2
131	A Multiâ€Functional Separator for Liâ€5 Batteries: WS ₂ @C Nanoflowers Catalyze the Rapid Recycling of Lithium Polysulfides by Polar Attraction. ChemElectroChem, 2022, 9, .	3.4	2
132	Reactive Dual Magnetron Sputtering: A Fast Method for Preparing Stoichiometric Microcrystalline ZnWO4 Thin Films. Surfaces, 2021, 4, 106-114.	2.3	1
133	Von der Verbrennung zum Herzschlag: Chemische TriebkrÄfte. Chemie in Unserer Zeit, 2004, 38, 10-23.	0.1	0
134	"Physical Chemistry of Solar Fuels Catalysis―— An Event for Early Career Researchers at the Max-Planck-Institute for Chemical Energy Conversion. ACS Energy Letters, 2016, 1, 353-355.	17.4	0
135	Photoelectrochemistry: Enhanced Photoresponse of FeS2 Films: The Role of Marcasite-Pyrite Phase Junctions (Adv. Mater. 43/2016). Advanced Materials, 2016, 28, 9656-9656.	21.0	0
136	Innenrücktitelbild: Probing CO ₂ Reduction Pathways for Copper Catalysis Using an Ionic Liquid as a Chemical Trapping Agent (Angew. Chem. 41/2020). Angewandte Chemie, 2020, 132, 18431-18431.	2.0	0
137	Innentitelbild: Nanoskaliger hybrider amorph/graphitischer Kohlenstoff als Schlüssel zur nähsten Generation von kohlenstoffbasierten Katalysatoren für oxidative Dehydrierungen (Angew. Chem.) Tj ETQq1 1 0	. 728⊕ 314 ı	rgBJT /Overlo
138	Deacon Process over RuO2 and TiO2-Supported RuO2. , 2010, , 517-528.		0
139	(Digital Presentation) Investigation of Reversal Tolerant Anode Catalysts Ageing during Start-up/Shut-Down Events on a PEM Fuel Cell. ECS Meeting Abstracts, 2022, MA2022-01, 1467-1467.	0.0	0